CONCRETE LIBRARY OF JSCE NO. 25, JUNE 1995

A UNIFIED PLASTIC MODEL FOR CONCRETE

(Translation from JSCE, Vol.24, No.496, August 1994)

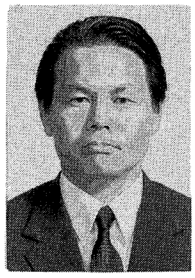

Tada-aki TANABE

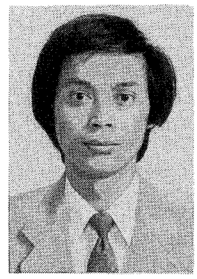

Zhishen WU

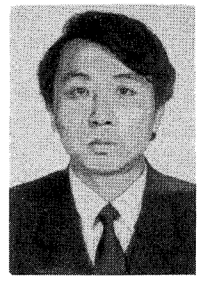

Guoxiong YU

The concrete models so far proposed have different criteria corresponding to different stress states. In this paper, a unified plastic model for concrete, in which only one criterion is used to describe the behavior of concrete under different stress states, is proposed. The proposed model treats the major nonlinear phenomena exhibited by concrete, such as cracking, shear transfer degradation, tension stiffening, and compressive strength reduction. By use of this model, the cumbersome considerations required in an analysis of concrete structures by other models can be eliminated.

Keywords: concrete, plasticity, load history, hardening, softening

---

T. Tanabe is a Professor of Civil Engineering at Nagoya University, Nagoya, Japan. He received his Doctor of Engineering Degree from University of Tokyo. He is the chairman of JCI Committee on the Thermal Stress of Massive Concrete Structures besides a member of various committees of JSCE, JCI and ACI. His main research is directed to the dynamic failure mechanism of RC structures besides the thermal stress.

Z. Wu is an Associate Professor of Civil Engineering at Ibaragi University, Hitachi, Japan. He received his Doctor of Engineering Degree from University of Nagoya in 1990. His research interests include computational modeling, failure mechanism and cracking properties of RC structures. He is a member of JSCE and JCI.

G. Yu is a Research Associate of Civil Engineering at Nagoya University, Nagoya, Japan. He received his Doctor of Engineering Degree from University of Nagoya in 1995. His research interests include nonlinear finite element analysis and failure mechanism of RC structures. He is a member of JSCE and JCI.

---

1. INTRODUCTION

Finite element software has recently found widespread use in analyzing reinforced concrete structures. However, to obtain reliable analytical results for structures made of materials with strongly softening behavior, careful attention is needed in certain respects: the need for a special numerical algorithm to deal with the phenomena of bifurcation and strain localization, and the need for a reasonable model of the material. So far, however, no constitutive model which can be used to describe the behavior of a material under various kinds of stress path with the same criterion has been available, and it is clear that already existing models are good at describing one aspect of the characteristics of a material but fail to describe the others.

Concrete, which is composite of aggregate and cement, differs from other materials and needs a special failure criterion to describe its unique characteristics: its tendency to fail in a brittle pattern or ductile pattern according to the stress state and the fact that its ductility can be increased and decreased by altering the compressive stress in the transverse direction. The Mohr-Coulomb and Drucker-Prager criterion are often used. However, there are some discrepancies between the analytical results achieved using these criteria and experimental measurements of concrete tensile behavior and tensile strength. To improve match, a tension-cutoff limit is used or a different kind of model is adopted, but it still seems that it is not possible to use a continuous function for the failure criterion.

Moreover, in the analysis of reinforced concrete structures, it is recognized that the major nonlinear factors are tension stiffening effect due to bond-slip behavior between the concrete and the reinforcement and concrete nonlinearities including compressive strength reduction due to transverse tensile strain, and shear transfer at a crack surface. A large number of experiments have been carried out, and the experimental observations have been used to develop different models for numerical analysis use according to different nonlinear phenomenon. However, we still lack a unified model that can deal with all these nonlinear factors in the same model. Recently, using plastic failure theory, the authors have made some progress in simulating the mechanism of stress transfer between cracks and some new results have been obtained. On the basis of this new knowledge, we propose a unified plastic model in this paper. In this model, the authors attempt to use a unified equation for the failure criterion of concrete. By adopting the concept of accumulated damage, this model is able to describe hardening behavior as well as softening behavior. This model eliminates the cumbersome considerations required in an analysis of reinforced concrete structures using other models.

2. TANGENTIAL CONSTITUTIVE MATRIX BASED ON THE ISOTROPIC HARDENING RULE

The present formulation essentially follows the basic outline of classical hardening plasticity theory[2] for the sake of simplicity. The subsequent failure surface is assumed to change size continuously depending on the damage accumulated in the concrete material, i.e., the failure surface is a function of the damage $\omega(W^p)$

$$f = f(\sigma_{ij}, \omega(W^p)) = 0 \tag{1}$$

where ω is the accumulated damage which is a function of W^p, W^p denotes the plastic work accumulated after the initial failure, and σ_{ij} denotes Cauchy's stress tensor.

Furthermore an independent function, i.e., the plastic potential function g is defined as

$$g = g(\sigma_{ij}, \omega(W^p)) = 0 \tag{2}$$

Generally, the application of the classical plasticity theory implies that the total strain rate comprises an elastic part and plastic part, as

$$\dot{\varepsilon}_{kl} = \dot{\varepsilon}^e_{kl} + \dot{\varepsilon}^p_{kl} \tag{3}$$

From the plastic potential g, the plastic strain rate tensor is assumed to be

$$\dot{\varepsilon}^p_{kl} = \dot{\lambda}\frac{\partial g}{\partial \sigma_{kl}} \tag{4}$$

where $\dot{\lambda}$ is non-negative multiplier which can be determined from the consistency condition during loading.

One the other hand, the elastic strain rate tensor $\dot{\varepsilon}^e_{kl}$ is assumed to be related to the stress rate tensor via the elasticity tensor D^e_{ijkl} as

$$\dot{\sigma}_{ij} = D^e_{ijkl}\dot{\varepsilon}^e_{kl} \tag{5}$$

The consistency condition $\dot{f} = 0$ can be expressed as

$$\dot{f} = \frac{\partial f}{\partial \sigma_{ij}}\dot{\sigma}_{ij} + \frac{\partial f}{\partial W^p}\dot{W}^p = 0 \tag{6}$$

where $\dot{W}^p$ can be written as

$$\dot{W}^p = \sigma_{ij}\dot{\varepsilon}^p_{ij} \tag{7}$$

Substituting Eqs.(3),(4),(5), and (7) into Eq.(6) and solving for $\dot{\lambda}$ yields

$$\dot{\lambda} = \frac{\frac{\partial f}{\partial \sigma_{ij}} D^e_{ijkl}\dot{\varepsilon}_{kl}}{\frac{\partial f}{\partial \sigma_{mn}} D^e_{mnpq}\frac{\partial g}{\partial \sigma_{pq}} + h} \tag{8}$$

with the definition

$$h = -\frac{\partial f}{\partial W^p}\sigma_{ij}\frac{\partial g}{\partial \sigma_{ij}} \tag{9}$$

Furthermore, the tangential constitutive matrix can be obtained using Eq.(10)

$$D_{ijkl} = D^e_{ijkl} - \frac{D^e_{ijtu}\frac{\partial f}{\partial \sigma_{rs}}\frac{\partial g}{\partial \sigma_{tu}} D^e_{rskl}}{\frac{\partial f}{\partial \sigma_{mn}} D^e_{mnpq}\frac{\partial g}{\partial \sigma_{pq}} + h} \tag{10}$$

As in the classical theory of plasticity, the subsequent yield surface can be expressed with the multiparameters $\xi_1, \xi_2, \cdots, \xi_i, \cdots$

$$f(\sigma_{ij}, \xi_1, \xi_2, \cdots, \xi_i, \cdots) = 0 \tag{11}$$

Here, this series of parameters is assumed to consist of unique functions of the damage parameter ω and are defined to characterize the shape and size of the yield surfaces. The initial loading surface is assumed to coincide with the elastic limit surface. The subsequent yield surface expands with the increase in inelastic strain during hardening. After the stress reaches the ultimate condition named the initial failure surface, the subsequent yield surface begins fall steadily in size until it reaches the final failure state, named the final failure surface.

The function $\partial f / \partial W^p$ can be elaborated, then, as

$$\frac{\partial f}{\partial W^p} = \left(\frac{\partial f}{\partial \xi_1} \frac{\partial \xi_1}{\partial \omega} + \frac{\partial f}{\partial \xi_2} \frac{\partial \xi_2}{\partial \omega} + \cdots + \frac{\partial f}{\partial \xi_i} \frac{\partial \xi_i}{\partial \omega} + \cdots \right) \frac{\partial \omega}{\partial W^p} \tag{12}$$

For more details of the hardening and softening of the failure surface, see references [3] and [4].

In the past, different theories were used in the concrete model according to the stress situation. Although a few[9] have attempted to adopt a unified criterion based on plastic theory, none can be correctly applied with respect to an arbitrary stress path. Therefore, different equations are generally used to describe the hardening and softening behavior separately, and application is complicated because of the need to deal with many parameters to describe the nonlinearity. In this research, a unified theory for different stress paths is achieved by defining, for convenience, a damage parameter which represents the accumulated damage due to progressive growth of the micro cracks etc., in the form

$$\omega = \frac{\beta}{\sigma_e \varepsilon_0} \int dW^p \tag{13}$$

where, σ_e is the effective stress defined later by Eq.(29), β is a material constant, and ε_0 is a constant fixed at $\varepsilon_0 = 0.002$.

3. MODIFIED DRUCKER-PRAGER FAILURE SURFACE

In previous work [3][4] , we used a Drucker-Prager failure surface to express concrete behavior under compressive loads. However, experience showed this still does not correctly express the tensile behavior as well as compressive behavior with the same values of characteristic parameters β and m. In particular, certain difficulties arose in calculating nonproportional tensile and compression stress paths. Hence, in this study, a modified Drucker-Prager Failure Surface as the expressed by Eq.(14) is adopted.

$$f = J_2 - (k_f - \alpha_f I_1)^2 + (k_f - \alpha_f \eta)^2 = 0 \tag{14}$$

Further, a similar expression for the plastic potential function is assumed:

$$g = J_2 - (k_g - \alpha_g I_1)^2 + (k_g - \alpha_g \eta)^2 = 0 \tag{15}$$

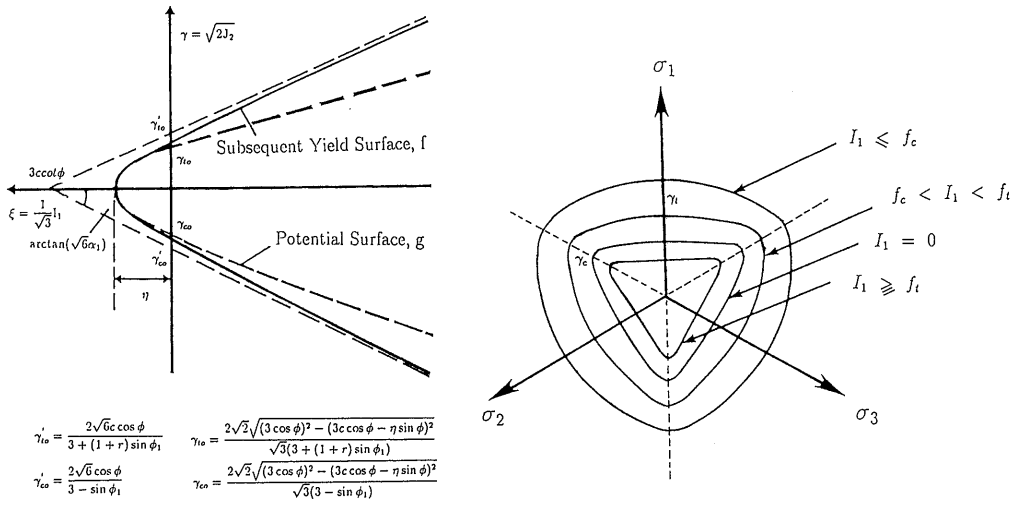

(a) Meridian Plane (b) Deviatoric Plane

Figure 1: Proposed Failure Surface

where $I_1 = \sigma_{kk}$ and $J_2 = \frac{1}{2}s_{ij}s_{ij}$ are the first invariant of stress tensor σ_{ij}, and the second invariant of deviatoric stress tensor s_{ij}, respectively, and α_f, k_f, α_g, and k_g are material constants defined by later equations.

The failure surface of Eq.(14) is shown in Fig.1. It is recognizable as having the Drucker-Prager surface as its asymptotic surface.

This Drucker-Prager failure surface is modified such that, when $I_1 \ll 0$, it gradually approaches the Drucker-Prager surface; on the other hand, when $I_1 > 0$, the failure surface on the meridian plane is a gradually changing curve, as shown by Fig.1(a). When I_1 increases, the tension meridian decreases faster than the compression meridian, so the failure surface gradually takes on the form of the Mohr-Coulomb failure surface. Figure 1 shows that the proposed failure surface has the general properties required, convexity, and the property required for concrete, that is, the failure surface on the deviatoric plane changes from a shape similar to a triangle (in tensile stress states) to a shape similar to a circle (in compression stress states).

Similar is the situation for the potential function.

According to the cohesion c, the internal friction angle ϕ, α_f, and k_f are defined as

$$k_f = \frac{6c\cos\phi}{\sqrt{3}(3+y\sin\phi_1)} \tag{16}$$

$$\alpha_f = \frac{2\sin\phi}{\sqrt{3}(3+y\sin\phi_1)} \tag{17}$$

where ϕ_1 is constant, $\phi_1 = 14°$, and the function y is defined as

$$y = \sqrt{a(\cos 3\theta + 1.00) + 0.01} - 1.10 \tag{18}$$

where $a = \frac{1}{2}r^2 + 2.1r + 2.2$, and

$$r = \begin{cases} 3.14 & (I_1 \leq f_c') \\ 2.93\cos\left(\frac{I_1}{f_c'}\pi\right) + 6.07 & (f_c' < I_1 \leq f_t) \\ 9.0 & (I_1 > f_t) \end{cases} \tag{19}$$

where $cos3\theta = 3\sqrt{3}J_3/2J_2^{\frac{3}{2}}$, and $J_3 = \frac{1}{3}s_{ij}s_{jk}s_{ki}$ is the third invariant of the stress tensor σ_{ij}.

Equation (18) is so determined that numerical simulations of two-dimension stress states are in good agreement with the experimental results by Kupfer. When $\theta = 0°, 60°$, y equals $1 + r$ and -1, respectively. Also, to describe the special characteristics of the concrete, a small value is used for the tensile meridian and big value for the compressive meridian; when I_1 decreases, the failure surface on the meridian plane changes gradually from a triangle to a circle. Figure 1(b) shows the deviatoric plane determined by Eqs (14) to (19), and this deviatoric plane is in agreement with experimental results.

The symbols ϕ and c are two strength parameters in the Mohr-Coulomb criterion, namely the so-called mobilized friction angle and mobilized cohesion. They are not constant, but depend on the plastic strain history through the damage parameter ω. In spite of the paucity of experimental data to support a definition of the damage parameter ω, we are able to say something about the dependence of ϕ and c on ω. In general, as the external force increases, a crack occurs and develops gradually in the concrete, and the concrete changes from its initial continuum state, to a granular state to which the resistance imposed by friction increases and that provided by cohesion decreases. Thus the value of ϕ should generally be an ascending function of ω, while c may be expected to be a descending function of ω. Possible relations for the hardening and softening model are suggested as follows (Fig.2).

$$c = c_0 \exp\left[-(m\omega)^2\right] \tag{20}$$

$$\phi = \begin{cases} \phi_0 + (\phi_f - \phi_0)\sqrt{2\omega - \omega^2} & \omega \leq 1 \\ \phi_f & \omega > 1 \end{cases} \tag{21}$$

where m is a material constant.

The symbols c_0, ϕ_0, and ϕ_f denote initial cohesion, initial internal friction angle, and final internal friction angle of the concrete, respectively. These relations are shown in Fig.2.

In a similar manner, we define

$$k_g = \frac{6c\cos\psi}{\sqrt{3}(3 + y\sin\phi_1)} \tag{22}$$

$$\alpha_g = \frac{2\sin\psi}{\sqrt{3}(3 + y\sin\phi_1)} \tag{23}$$

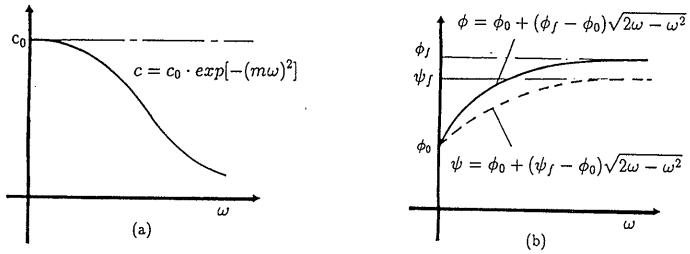

Figure 2: Material Parameters c, ϕ, and ψ Affected by Damage ω

$$\psi = \begin{cases} \phi_0 + (\psi_f - \phi_0)\sqrt{2\omega - \omega^2} & \omega \leq 1 \\ \psi_f & \omega > 1 \end{cases} \tag{24}$$

with a particular mobilized dilatancy angle ψ. Note that for $\phi = \psi$, we have $f = g$ and the classical associated flow rule is recovered.

The symbol η in Eq.(14) and Eq.(15) is a tension behavior factor. As the accumulated damage increases, tensile debonding occurs. This can be expressed as

$$\eta = \eta_0 \exp\left(-\frac{\omega}{b}\right) \tag{25}$$

in which b is a constant varying with the reinforcement ratio, for plain concrete, $b = 0.06$, and η_0 is the tensile strength on the hydrostatic axis, which is also close to the uniaxial tensile strength.

By using a hyperbolic function for the failure surface, smooth tracing of the stress-strain relation from tension to compression during nonproportional loading is possible.

4. THE ASSOCIATED FLOW RULE

4.1 Hardening and the Deviation of $\frac{\partial f}{\partial \dot{W}^p}$

The associated flow rule is commonly applied for practical reasons. In the associated flow rule, it is interesting to note that the plastic work rate is

$$\dot{W}^p = \sigma_{ij}\dot{\varepsilon}^p_{ij} = \dot{\lambda}\sigma_{ij}\frac{\partial f}{\partial \sigma_{ij}} \tag{26}$$

The scalar function $\dot{\lambda}$ can be obtained by squaring each of the terms in Eq.(4) and adding, as

$$\dot{\varepsilon}^p_{ij} \cdot \dot{\varepsilon}^p_{ij} = \lambda^2 \frac{\partial f}{\partial \sigma_{ij}}\frac{\partial f}{\partial \sigma_{ij}} \tag{27}$$

The effective plastic strain rate is defined simply as

$$\dot{\varepsilon}_p = \sqrt{\dot{\varepsilon}^p_{ij} \cdot \dot{\varepsilon}^p_{ij}} \tag{28}$$

Then, the effective stress is defined using the plastic work increment as

$$\sigma_e = \frac{\dot{W}^p}{\dot{\varepsilon}_p} = \frac{\sigma_{ij}\dot{\varepsilon}^p_{ij}}{\dot{\varepsilon}_p} \tag{29}$$

According to the preceding discussion, $\partial f/\partial W^p$ in Eq.(12) for the modified Drucker-Prager criterion can be rewritten as

$$\begin{aligned}\frac{\partial f}{\partial W^p} &= \left(\frac{\partial f}{\partial \alpha_f}\frac{\partial \alpha_f}{\partial \omega} + \frac{\partial f}{\partial k_f}\frac{\partial k_f}{\partial \omega} + \frac{\partial f}{\partial \eta}\frac{\partial \eta}{\partial \omega}\right)\frac{\partial \omega}{\partial W^p} \\ &= 2\left[(I_1-\eta)(k_f-\alpha_f(I_1+\eta))\frac{\partial \alpha_f}{\partial \omega} + \right. \\ &\left. \alpha_f\,(I_1-\eta)\frac{\partial k_f}{\partial \omega} - \alpha_f(k_f-\alpha_f\eta)\frac{\partial \eta}{\partial \omega}\right]\frac{\partial \omega}{\partial W^p}\end{aligned} \tag{30}$$

where,

$$\frac{\partial \alpha_f}{\partial \omega} = \frac{2\cos\phi}{\sqrt{3}(3+y\sin\phi_1)}\frac{\partial \phi}{\partial \omega} \tag{31}$$

$$\frac{\partial k_f}{\partial \omega} = \frac{-6c\sin\phi}{\sqrt{3}(3+y\sin\phi_1)}\frac{\partial \phi}{\partial \omega} - \frac{12c_0m^2\omega}{\sqrt{3}(3+y\sin\phi_1)}e^{-(m\omega)^2}\cos\phi \tag{32}$$

and

$$\frac{\partial \eta}{\partial \omega} = -\frac{\eta_0}{b}\exp\left(-\frac{\omega}{b}\right) \tag{33}$$

Moreover,

$$\frac{\partial \phi}{\partial \omega} = \begin{cases} \dfrac{(1-\omega)(\phi_f-\phi_0)}{\sqrt{2\omega-\omega^2}} & \omega \le 1 \\ 0 & \omega > 1 \end{cases} \tag{34}$$

$$\frac{\partial \omega}{\partial W^p} = \frac{\beta}{\sigma_e\varepsilon_0} \tag{35}$$

4.2 Loading Criterion

In the softening region, plastic loading and elastic unloading are considered to occur at the same level. Thus, the commonly used loading criterion for work hardening is invalid in this model. Certain modifications are needed and the modified loading criterion shown in Fig.3 is defined as

Elastic unloading

$$\frac{\partial f}{\partial \sigma_{ij}} \Delta \sigma_{ij}^{e} \geq 0 \qquad (36)$$

Plastic loading

$$\frac{\partial f}{\partial \sigma_{ij}} \Delta \sigma_{ij}^{e} < 0 \qquad (37)$$

here

$$\Delta \sigma_{ij}^{e} = D_{ijkl}^{e} \Delta \varepsilon_{kl} \qquad (38)$$

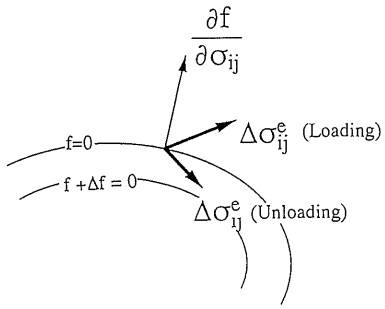

Figure 3: Loading Criterion

5. STUDIES OF INITIAL PARAMETERS AND MATERIAL CONSTANTS

5.1 Effects on the Model

First, we investigate the effect on concrete behavior of changing the initial parameters and the material constants. From Eqs.(16),(17),(22), and (23), we can see that ϕ_1, ϕ_0, and ε_0 have fixed values. First, we let $\phi_1 = 14°$, $\phi_0 = 5°$, and $\varepsilon_0 = 0.002$, which has no significant effect on the behavior of the model, and study the effects on concrete behavior of changing the following six initial parameters or material constants.

1. The Effect of Changing c_0 (Initial Cohesion)

   In the Drucker-Prager failure criterion, the initial cohesion parameter c_0 is an important influence on the behavior of the concrete. In this unified model, as shown by Fig.4, when the c_0 becomes bigger, the compressive strength increases but the corresponding change in compressive strain is insignificant. On the other hand, changing c_0 has little effect on the tensile strength and the corresponding tensile strain. The reason for this is that the rate of damage accumulation under tension is much bigger than under compression, since under tension when the damage procedure begins, the cohesion c becomes very small soon.

2. The Effect of Changing ϕ_f (Maximum Internal Friction Angle)

   The internal friction angle is another important factor in the Drucker- Prager failure criterion. In this unified model, as shown in Fig.5, when ϕ_f increases, the compressive strength and the corresponding compressive strain become bigger. A comparison with experimental results shows that a value of ϕ_f between 30° to 40° is suitable. Now, we have two parameters, ϕ_f and c_o, affecting the compressive behavior of the concrete, so for simplicity, we should fix one and change the other alone. Since changing ϕ_f affects concrete behavior less than c_0, in this research, ϕ_f is fixed at 35°. On the other hand,

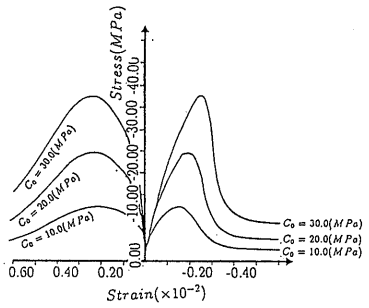

Figure 4: The Effect on Concrete Behavior of Changing c_0

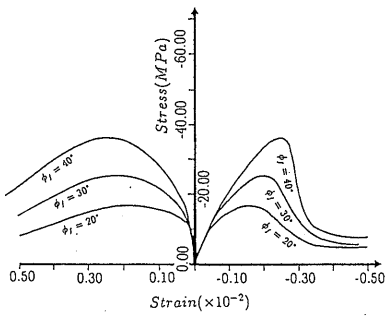

Figure 5: The Effect on Concrete Behavior of Changing ϕ_f

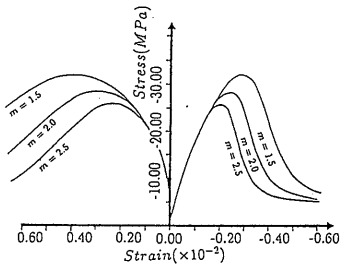

Figure 6: The Effect on Concrete Behavior of Changing m

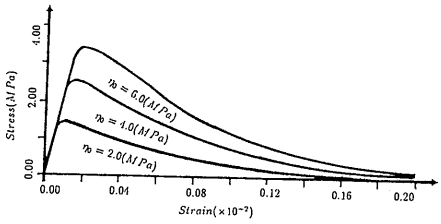

Figure 7: The Effect on Concrete Behavior of Changing η_0

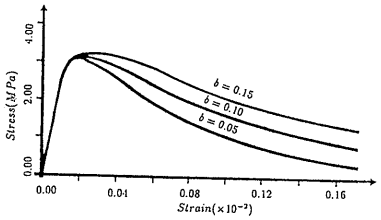

Figure 8: The Effect on Concrete Behavior of Changing b

changing ϕ_f has little effect on the tensile strength and also the corresponding tensile strain. This is because, under tension, even when the tensile stress reaches a maximum value, the maximum internal friction angle is almost unchanged near ϕ_0.

3. The Effect of Changing m (Material Constant)

   m is the material constant in Eq.(20) and has effect on the softening behavior (descending branch) of cohesion c. As shown in Fig.6, m has a significant effect on the compression behavior of concrete; the bigger m is, the lower the compressive strength and the corresponding compressive strain are. On the other hand, m has little effect on tensile strength or the corresponding tensile strain. From simulation results, and in particular a comparison with the shape of curve in the uniaxial compressive experiment, it seems suitable to make $m = 1.0$.

4. The Effect of Changing β (Material Constant)

   β is an important material constant in defining the damage parameter (Eq.(13)). In terms of compressive behavior, changing β has little effect on compressive strength but

does affect the corresponding compressive strain. Under tension, it has an effect on the softening branch but not on the tensile strength or the corresponding tensile strain. A comparison with Kupfer's experimental results indicates that $\beta = 0.40$ is a suitable choice.

5. The Effect of Changing η_0 (Material Constant)

   η is the tensile strength on the hydrostatic axis and η_0 is the initial value of η (Fig.1(a)). As the concrete damage increases, η decreases from η_0 gradually. The effect on compressive strength and the corresponding strain of changing η_0 is so small that it can be ignored. But, as shown by Fig.7, η_0 is an important factor affecting the tensile behavior of concrete.

6. The Effect of Changing b (Material Constant)

   The effect of changing the material constant b on the compressive behavior of concrete is so small that it can be ignored. However, it has a significant effect on the softening path, though little effect on the tensile strength, as shown in Fig.8. For plain concrete, after comparing with sufficient experiment data, $b = 0.006$ is considered an appropriate choice. In the case of reinforced concrete (such as reinforced concrete panels), there is a type of phenomenon called "Tension Stiffening", due mainly to the bond-slipping behavior between concrete and reinforcement. Although a large amount of research has been done, no satisfactory conclusion has been reached. According to past experiments and research results, reinforcement ratio has a large effect on the "Tension Stiffening" phenomenon, it is possible that with this concrete model, a value of b should be identified to reflect this phenomenon.

From this examination of each parameter and material constant, it can be concluded that this unified concrete model is able to treat the compressive behavior (determined by the value of c_o) and the tensile behavior (determined by the values of η_o and b) of concrete with one set of parameters and material constants using only one failure criterion.

5.2 The Relationship Between $f_c' \sim c_0$ and $f_t \sim \eta_0$

From the numerical simulation discussed in the Section 5.1, it can be concluded that the most suitable values for ϕ_f, m, and β are $\phi_f = 35°$, $m = 1.0$, and $\beta = 0.4$, respectively. The factor affecting the behavior of compressive strength is the initial parameter c_0, while the factor affecting the tensile strength is the material constant η_0.

Figure 9 shows the relationship between c_0 and compressive strength, while Fig.10 shows η_0 and the tensile strength relation. For commonly used concrete, tensile strength seldom exceeds 4.0 MPa, so the value of η_o should be lower than 10.0 MPa. In practical use, we can determine c_0 and η_0 from the compressive strength and the tensile strength using Figs. 9 and 10.

6. COMPARISON WITH EXPERIMENTAL RESULTS

6.1 Comparison with Kupfer's Experiment

Kupfer has carried out experimental studies on the concrete specimens under various kinds of proportional loading in two dimensions [5]. Here, we compare the numerical simulation results obtained using this unified model with the Kupfer's experimental results, as shown in Fig.11. c_0 and η_0 are determined by the method stated in Section 5.2. From Fig.11, it can be seen that this model gives good results in not only uniaxial but also biaxial numerical simulations.

6.2 Comparison with Petersson's Experiment

A numerical simulation of uniaxial tension is also carried out for comparison with Petersson's experimental results [6], as shown in Fig.12. As discussed above, η_0 and b are the two most

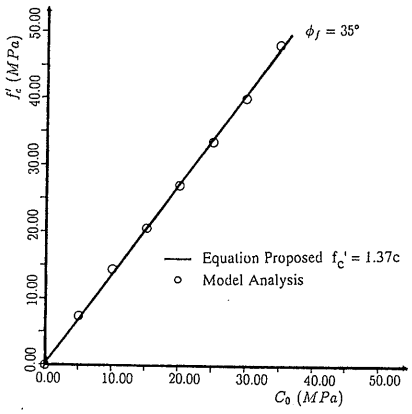

Figure 9: The Relation between c_0 and Compressive Strength f_c'

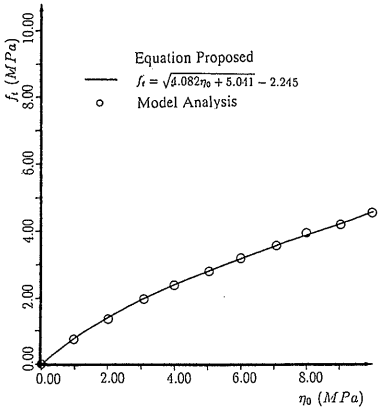

Figure 10: The Relation between η_0 and Tensile Strength f_t

Kupfer (1969) $E_c = 3.25 \times 10^4 MPa$ $\eta_0 = 3.8MPa$ $\phi_t = 35°$ $m = 1.0$ $\epsilon_0 = 0.002$
$c_0 = 24.0MPa$ $\upsilon = 0.22$ $\phi_0 = 5°$ $\beta = 0.40$ $b = 0.06$

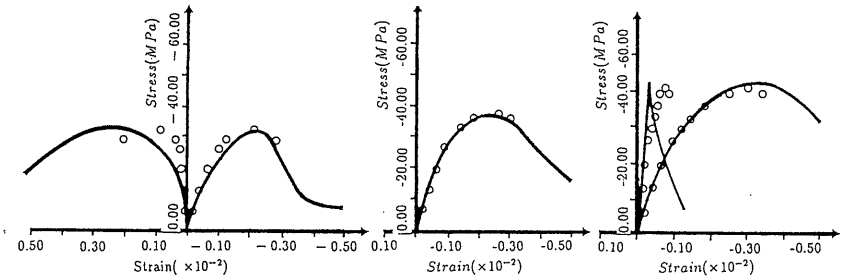

(a) Uniaxial Compression (b) $(\frac{\sigma_1}{\sigma_2} = \frac{-1}{-1})$ (c) $(\frac{\sigma_1}{\sigma_2} = \frac{-1}{-0.52})$

Figure 11: Comparison with Kupfer's Experiment

Petersson (1981) $E_c = 1.72 \times 10^4 MPa$ $\upsilon = 0.22$ $\phi_0 = 5°$ $\beta = 0.40$ $b = 0.05, 0.06$
$c_0 = 24.0MPa$ $\phi_t = 35°$ $m = 1.0$ $\epsilon_0 = 0.002$

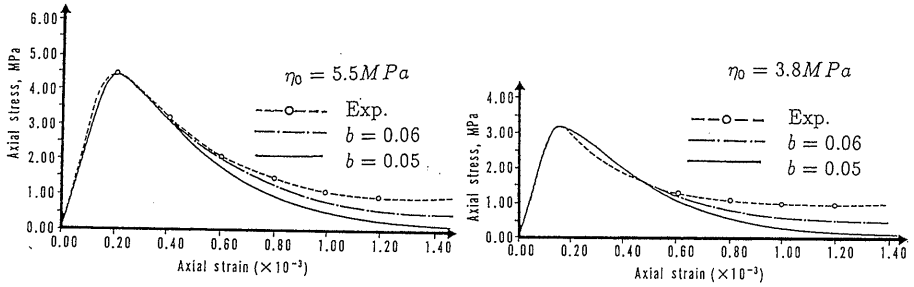

Figure 12: Comparison with Petersson's Experiment

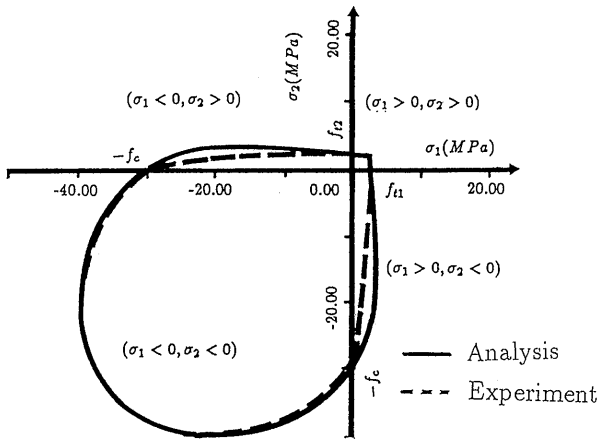

Kuffer(1969)

$E_c = 3.25 \times 10^4 MPa$ $\beta = 0.40$ $r = 3.14$
$\upsilon = 0.22$ $\phi_0 = 5°$ $\epsilon_0 = 0.002$
$c_0 = 24.0 MPa$ $\eta_0 = 5.5$
$\phi_t = 35°$ $m = 1.0$ $b = 0.06$

Figure 13: The Strength Envelope under Biaxial Stress States

important parameters affecting the tensile behavior of concrete. η_0 is determined by the method described in Section 6.2, while $b = 0.06$ is assumed for plain concrete. Figure 12 shows that this model gives good results.

6.3 Strength Envelope under Biaxial Stress State

It is difficult to obtain a strength envelope which closely fits experiment results using existing concrete models. Here, strength envelopes under biaxial stress, obtained by our unified concrete model and from Kupfer's experiments [5], are shown on Fig.13. In the compression-compression, tension-tension regions the analysis curve is in agreement with the experiment results, but in the tension-compression region there is some difference. This requires further investigation.

6.4 Strength Reduction by Transverse Tensile Strain

Many experiments have been carried out with regard to this problem (Petersson, P.E.[6], Cervenka, V.[7], and Vecchio, F.J. and Collins, M.P.[8]). The phenomenon is interpreted as a the strength reduction under compressive loading in a stress state where transverse tensile stress or strain is maintained.

To examine how this phenomenon is handled by the model, some numerical examples are calculated. Concrete which has a uniaxial compressive strength of 26.5MPa and a uniaxial tensile strength of 2.5MPa is examined.

First, the concrete is subjected to uniaxial force to a extent of damage accumulated which is indicated by a tensile strain given, and then, from this state at a certain level of damage, compressive force is applied in the vertical direction until failure. Figure 14(b) shows the compressive stress in the vertical direction and the corresponding compressive strain relations with respect to various values of tensile strain in the horizontal direction. Figure 14(c) shows the behavior of uniaxial tension when the parameters shown are used. As discussed before, constant b is an important influence on the tension stiffening behavior of reinforced concrete, and in this example it is assumed that the concrete has some amount of reinforcement in the horizontal direction, so $b = 0.1$. For details of how this model deals with the tension stiffening phenomenon, see reference [4]. The strength reduction in this case is plotted against the curves proposed by Vecchio and Collins [8] and by Cervenka [7] in Fig.14(d). From Fig.(b) and (d),

$E_c = 2.49 \times 10^4 MPa$ $\eta_0 = 4.3MPa$ $\phi_t = 35°$ $m = 1.0$ $\epsilon_0 = 0.002$
$c_0 = 22.0MPa$ $\upsilon = 0.22$ $\phi_0 = 5°$ $\beta = 0.30$ $b = 0.10$

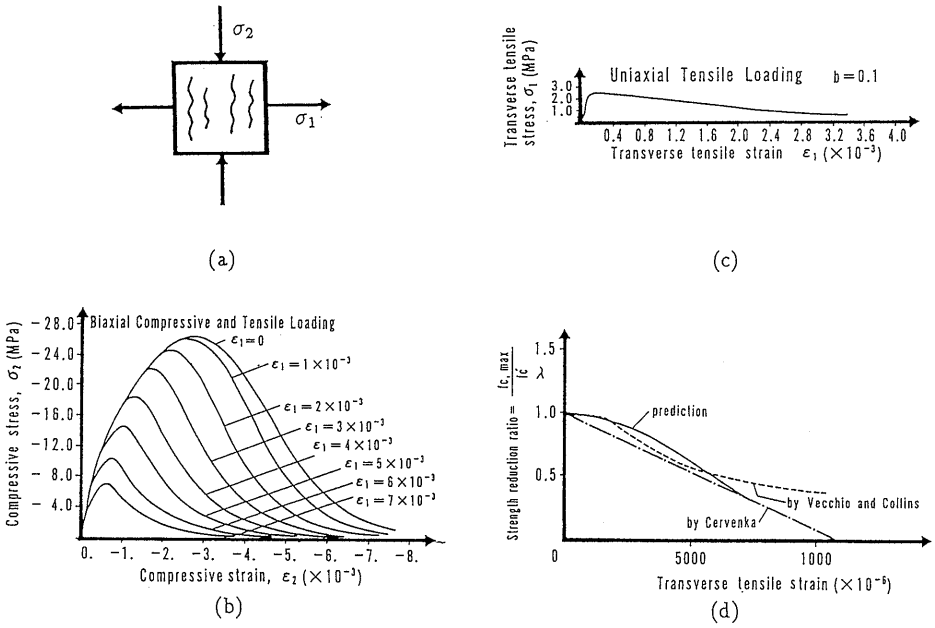

Figure 14: Comparison of Strength Reduction Ratios

it can be seen that as the tensile strain increases in the horizontal direction, the compressive strength and the corresponding compressive strain decrease.

As the numerical simulations show, this model makes it possible to describe strength reduction due to the transverse tensile strain phenomenon. Thus it is possible using this model to analysis reinforced concrete structures with preexisting crack under the cyclic loading such as earthquake forces.

Although, discussion in this paper is limited to the two-dimensional case, application of this model to three dimensions is also valid.

7. CONCLUSION

To describe the special characteristics of concrete, the authors have proposed a failure criterion which is defined by several parameters related to the friction angle, cohesion, and accumulated damage. In this model, using the three parameters c, ϕ, and η, tensile and compressive behavior as well as the hardening and softening behavior can be described using only one equation (the unified failure criterion). Moreover, the authors have developed a theory to describe the process of damage as stress is transferred between discontinuous surfaces inside concrete by using the

method described in this paper [1]. This model can treat the major nonlinear phenomena occurring in concrete, such as cracking, shear transfer degradation, tension stiffening, and compressive strength reduction. By using this model, the cumbersome considerations needed in the analysis of concrete structures by other models can be eliminated.

The application of this model to more complicated stress paths will be reported in near future publications. Regarding other problems such as strain localization and the size effect, more research is needed. They can probably be solved by introducing such concepts as fracture energy and virtual viscosity into the model. Problems such as the slight reduction in elastic properties when the material undergoes unloading after some damage is accumulated, and the description of dynamic properties when the material undergoes damage will be adopted as research topics in the future.

References

[1] Wu, Z.S., Farahat, A.M. and Tanabe, T., "Modeling of Concrete Discontinuities with Dilatancy and Surface Degradation", Proceedings of the Japan Society of Civil Engineers, Vol.20, No.472, pp.119-130, 1993.

[2] Chen, W.F., "Plasticity in Reinforced Concrete", McGraw-Hill, New York, 1982.

[3] Wu, Z.S. and Tanabe, T., "A Hardening /Softening Model of Concrete Subjected to Compressive Loading", Journal of Structural Engineering, Architectural Institute of Japan, Vol.36B, pp.153-162, March 1990.

[4] Tanabe, T. and Wu, Z.S., "Strain Softening under Biaxial Tension and Compression", IABSE Col. Stuttgart, pp.623-636, 1991.

[5] Kupfer, H., Hilsdorf, H.K. and Rusch, H., "Behavior of Concrete under Biaxial Stresses", ACI Journal, Vol.66, No.8, pp.656-636, Aug. 1969.

[6] Petersson, P.E., "Crack Growth and Development of Fracture Zone in Plane Concrete and Similar Materials", Report No. TVBM-1006,k Lund Institute of Technology, Dec. 1981.

[7] Cervenka, V., "Constitutive Model for Cracked Reinforced Concrete", ACI Journal, Vol.82, No.6, pp.877-882, Nov.-Dec. 1985.

[8] Vecchio, F.J. and Collins, M.P., "The Modified Compression- Field Theory for Reinforced Concrete Elements Subjected to Shear", ACI Journal, Vol.83, No.2, pp.219-281, Mar.-Apr. 1986.

[9] Pramono, E. and Willam, K., "Fracture Energy- Based Plasticity Formulation of Plain Concrete", Journal of Engineering Mechanics, ASCE, Vol.115, No.6, pp.1183-1204, June 1989.

[10] Miyahara, T., Kawakami, T. and Maekawa, K., "Nonlinear Behavior of Cracked Reinforced Concrete Plate Element under Uniaxial Compression", Journal of JSCE, No.378, Vol.6, pp.249-258, Feb. 1987.

[11] Wu, Z.S., Hoshikawa, H. and Tanabe, T., "Tension Stiffness Model for Cracked Reinforced Concrete", Journal of Structural Engineering, ASCE, Vol.117, No.3, pp.715-732, March 1991.